

Fabrication and Reporting Guidelines and Transference Number Correction in Composite Polymer Electrolyte-Based Lithium-Ion Batteries

Rajan Jose* and Chun-Chen Yang*

All-solid-state batteries (ASSBs) using composite polymer electrolytes (CPEs) are a promising technology for next-generation energy storage. These electrolytes combine an inorganic solid electrolyte (filler) and a lithium source dispersed in a polymer electrolyte matrix to achieve a balance between ionic conductivity and mechanical flexibility. The progress in developing material combinations for CPEs is significant; however, the fabrication and reporting of ASSBs by various laboratories considerably vary, thereby making a direct comparison of the results tedious. Recommended standard procedures are therefore necessary to align the research on ASSBs for a common goal. By analyzing various reports, a set of guidelines for the fabrication, testing,

and reporting of ASSBs is proposed. Besides, ASSBs employing CPEs often suffer from rapid capacity fade, typically failing after a few hundred charge/discharge cycles. A critical issue underlying the failure of ASSBs could be an overestimation arising from the disparity between experimentally measured average ionic conductivity and transference numbers and the local ionic transport properties within the electrolyte. This perspective also discusses the limitations arising from an unrealistic averaged ionic conductivity, the role of lithium-ion transfer cross sections, and potential remedies to improve long-term battery performance. Mathematical models and experimental evidence supporting these arguments are also presented.

1. Introduction

The liquid electrolytes (LEs) in the present-day lithium-ion battery technology and the associated safety issues arising from the low flashpoints of electrolyte components have triggered intensive research on solid electrolytes recently. The conventional LE, composed of a lithium salt (LiPF_6) dissolved in a mixture of organic carbonates, many of which have a flashpoint in the 16–25 °C range, has reported many accidents via explosion. The Joule heating during the battery operation and the associated temperature rise above the flash points lead to an explosion in certain cases despite the significant developments in the battery management systems. Three types of solid electrolytes have been proposed, viz., i) inorganic oxide or sulfide solid electrolytes such as NASICON-type $\text{Li}_{1+x}\text{Al}_x\text{T}_{2-x}(\text{PO}_4)_3$ (LATP) with a room temperature ionic conductivity (σ) of $\approx 0.27 \times 10^{-3} \text{ S cm}^{-1}$,^[1] garnet type $\text{Li}_7\text{La}_3\text{Ta}_2$ (LLZO) ($\sigma \approx 10^{-4}-10^{-3} \text{ S cm}^{-1}$),^[2,3] perovskite-type $\text{Li}_3\text{La}_{2/3-x}\text{TiO}_3$

(LLTO) ($\sigma \approx 10^{-3} \text{ S cm}^{-1}$),^[4,5] LISICON-type $\text{Li}_{4-x}\text{Ge}_1\text{xP}_x\text{S}_4$ (LGPS) ($\sigma \approx 2.2 \times 10^{-3} \text{ S cm}^{-1}$),^[6] argyrodite-type $\text{Li}_{10}\text{GeP}_2\text{S}_{12}$ (LGPS),^[7] and their variety of doped analogs; ii) polymer/polymer matrix such as PEO, PVDF-HFP with appropriate plasticizers and lithium salts with $\sigma \approx 10^{-4}-10^{-6} \text{ S cm}^{-1}$; and iii) composite polymer electrolytes (CPEs) in which the inorganic solid electrolytes are dispersed in polymer electrolytes with or without the addition of lithium salts with $\sigma \approx 10^{-2}-10^{-3} \text{ S cm}^{-1}$. These three types have their relative merits and drawbacks, for example, (i) the inorganic compounds are rigid and poorly percolate with the inorganic electrodes (such as NCM, LFP, or graphite) despite their higher ionic conductivity and ii) polymers electrolytes have high a degree of flexibility and but with inferior ionic conductivity.

The CPEs have been seen as the best compromise between the properties and the drawbacks. In CPEs, the lithium-ion conduction occurs through three main pathways, viz., i) through the amorphous regions of the polymer, ii) via the ion hopping between the interstitial sites of the inorganic solid electrolyte, and iii) through the polymer–inorganic interface.^[8,9] A larger transport through the polymer–inorganic interface is preferred as it can create a space charge layer to modify the local ion concentration and mobility, if suitable percolation networks could be established. Further, such an interface facilitates ion dissociation due to synergistic interaction between the lithium salt (such as lithium bis(trifluoromethanesulfonyl)imide, LiTFSI) and the surface of the inorganic solid electrolyte through Lewis acid–base interactions. This possibility has been recently explored to fabricate CPEs with $\sigma \approx 1 \times 10^{-3} \text{ S cm}^{-1}$ by incorporating a cation-deficient inorganic solid electrolyte ($(\text{La}_{0.7}\text{Sr}_{0.3})_{0.97}\text{TiO}_3$) into a polymer matrix (PVDF-HFP).^[10] The negatively charged cation defects intensified the Li-ion adsorption at the surface of the

R. Jose, C.-C. Yang
Battery Research Center of Green Energy
Ming Chi University of Technology
New Taipei City 24301, Taiwan
E-mail: rjose@umpsa.edu.my
ccyang@mail.mcut.edu.tw

C.-C. Yang
Department of Chemical Engineering
Ming Chi University of Technology
New Taipei City 24301, Taiwan, R.O.C.

C.-C. Yang
Department of Chemical and Materials Engineering & Center for Sustainability and Energy Technologies
Chang Gung University
Taoyuan City 333, Taiwan, R.O.C.

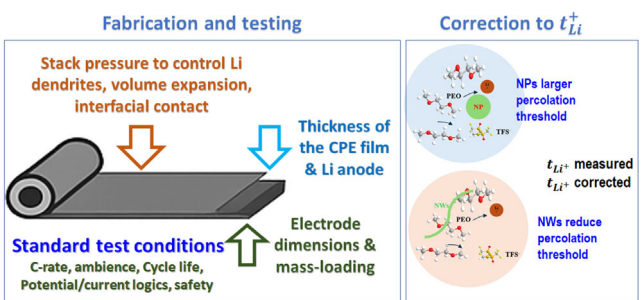


Figure 1. Schematics showing the focus of the study.

inorganic electrolytes and established a continuous ultrafast Li-ion transport network.^[10] Despite these advancements in understanding the ion conduction mechanism and improving the performance with appropriate materials modifications, batteries employing CPEs routinely suffer from rapid capacity fade, typically failing after a few hundred charge/discharge cycles.

The research on CPEs has been enormous; a search in the Scopus database using the keywords "composite polymer electrolyte" during April 2025 browsed over 8200 articles (excluding reviews, conference papers, book chapters, etc.) with nearly 1000 papers per year recently. These studies using diverse choices of materials brought in impressive lab-scale devices; however, a literature review reveals significant heterogeneity in the data reporting. A standard protocol for device fabrication and testing has not been established. Another critical issue underlying this failure is the disparity between experimentally measured average ionic conductivity and transference numbers and the local ionic transport properties within the electrolyte. This Perspective, therefore, discusses i) standard procedures for device fabrication, testing, and acceptable limits of physical quantities as well as ii) the limitations arising from an unrealistic averaged ionic conductivity, the role of lithium-ion transfer cross-sections, and potential remedies to improve long-term battery performance (Figure 1). We provide mathematical models and experimental evidence from the published literature supporting these arguments. This study is concluded in Section 4.

2. Recommended Procedure for All-Solid-State Battery Fabrication and Testing

As the rationale for developing the CPE is to replace the liquid electrolytes in the commercial lithium-ion battery with a safer solid analog, the standard fabrication and testing protocols are expected to follow a commercial standard. While the all-solid-state batteries (ASSBs) are still under development at the laboratory level, a set of guidelines to be followed to fabricate and test the battery for meaningful comparison and benchmarking of the technology development. Most works reported on ASSBs are on half-cell coin cell configuration with, typically, thick (200–400 µm) lithium metal plate as the counter and the reference electrodes reporting lithium diffusion coefficients and transference numbers as the characteristic of the CPEs and specific capacities, rate capabilities, cycling stabilities, and coulombic efficiencies as

the device performance indicators. A few works attempted to track the performance of the electrodes during cycling through devices with separate reference electrodes.^[11] Otherwise, the performances are usually validated using electrochemical impedance spectroscopy, as well as evaluating the chemical and morphological structures of the cycled electrodes. A full cell, even in coin cell configuration, is rarely reported and, together with their limited cathode mass-loading (areal capacity <0.5 mAh cm⁻²), makes the research results far from real devices (areal capacity ≈3–4 mAh cm⁻²). In the following, we list a meaningful standard protocol for the fabrication and testing of ASSBs such that the progress in this area could be benchmarked.

A pouch cell in the 3 × 4 cm dimensions with mass-loading in the 15–20 mg cm⁻² range. Pouch cells are advantageous over cylindrical cells, particularly when application volume and form factor flexibility are critical.^[12,13] Pouch cells make more efficient use of space due to their prismatic shape and flexible packaging. They lack the rigid metal casing found in cylindrical cells, which reduces unused volume and allows higher packing efficiency, which is ideal for applications where space is at a premium, such as smartphones, laptops, and electric vehicles. Besides, unlike cylindrical cells, which come in fixed sizes (e.g., 18 650 and 21 700), pouch cells can be customized in terms of size and shape. This flexibility makes them suitable for products with unique or irregular internal geometries, such as wearable devices or drones. In addition, the absence of a heavy metal casing can reduce the overall weight of pouch cells, improving the weight-to-energy ratio. This is especially beneficial in electric vehicles and portable electronics, where weight directly impacts performance and efficiency; pouch cells offer better coulombic and energy efficiencies.^[14,15] Moreover, pouch cells show better thermal performance as they tend to dissipate heat more evenly because of their flat surfaces, reducing the risk of hotspots and improving overall thermal management in large battery packs.^[15,16] Also, for the same materials and energy footprints, pouch cells can often store more energy than cylindrical counterparts, which simplifies battery pack design and reduces the number of cells needed.

The thickness of the CPE film is to be <100 µm. Thicker solid electrolytes in ASSBs increase internal impedance and reduce energy density, while thinner electrolytes improve performance due to smaller volume and reduced diffusion path.^[17–19] Reducing electrolyte thickness is crucial for high energy density, but it can also increase the risk of cracks. In ASSBs, keeping the CPE film below 100 µm (ideally in the 30–50 µm range) improves ionic conductivity, enhances energy density, ensures better electrode-electrolyte contact, and can still suppress dendrites if mechanically robust, thereby making it a practical and performance-driven design choice.

Lithium metal thickness of <20 µm in the lithium metal batteries: The optimal thickness in many cutting-edge lithium metal battery designs is 15–20 µm for better lithium utilization, reduced dendrite formation, optimized ion transport, as well as balancing energy density, safety, and cycle life.^[20] Further, thin lithium foils contribute to lighter batteries and enable higher energy density and improved conduction, leading to faster charging speeds and more stable operation.

Stack pressure to control dendrite formation, volume expansion, and interfacial contact: The mechanical force for maintaining the contact between the electrode and the solid electrolyte, referred to as stack pressure, is an important parameter for their performance and stability.^[21–23] Insufficient pressure to stack them leads to poor contact and high interfacial resistance, whereas excessive pressure results in lithium dendrite formation or material deformation. Therefore, an optimum stack pressure is required for safer operation for longer charge/discharge cycles while maintaining high capacity. Stack pressure can be applied via two categories, fixed displacement and constant pressure; systematic studies reveal that constant pressure devices offer better performance and more consistent pressure during the cell cycling.^[24]

The typical stack pressure applied to the commercial lithium-ion batteries during fabrication generally ranges in the 10–100 kPa, depending on the applications,^[25] which minimizes the risk of lithium dendrites forming and puncturing the separator, especially in lithium-metal or high-energy lithium-ion chemistries. Similar pressure helps suppress excessive swelling (volume change) upon electrochemical cycling, ensuring cell integrity over many cycles, ensuring better contact between the electrode and current collector, reducing internal resistance, and improving performance consistency. The effect of applied pressure on the key performance indicators of NMC622||Li cells (Li foil thickness ≈300 µm) fabricated using cross-linked polyethylene oxide as well as cross-linked cyclodextrin grafted poly(caprolactone) as solid polymer electrolytes studied by Roering et al.^[26] revealed a trade-off between rate capability and membrane deformation if the pressure is ≤ 43 kPa, which is considerably lower and more practical compared to cells employing ceramic electrolytes with external pressure ≥ 5 MPa. Nevertheless, a recent study employing a molecular ionic composite polymer electrolyte containing an ionic polymer and lithium salt used a stack pressure of ≈ 200 kPa for coin cells and 1 MPa for pouch cells and cycled up to 100 cycles with $>95\%$ capacity retention.^[27] The polymer component in the CPEs considerably reduces the stack pressure requirements. Therefore, considering the above

studies, the stack pressure for composite polymer electrolyte could have values in the range 100 kPa–5 MPa, depending on their chemical composition, where the lower limit is for the solid (filler)-in-polymer case and the upper limit for the polymer-in-solid (filler) case. Nevertheless, a stack pressure optimization to be routinely undertaken to ensure that the cell failure is not due to mechanical reasons.

Testing of lithium metal pouch cells fabricated using CPE with a standard protocol is relatively unaddressed, and the current laboratory practices are not worthwhile for real-world applications. In Table 1, we compare the current laboratory practices and a recommended testing protocol.

The majority of the published papers using CPEs for ASSBs are on the evaluation of their materials properties using coin cells toward the proposed use. Primarily, the testing at the laboratory ambience is with no control of temperature or humidity, the pressure applied to fabricate the coin cell has no set standards, and the test results with the best cycling conditions (which are mostly at low C-rates and current densities) are reported in the published papers. Set guidelines, as shown in Table 1, are required for the safety, performance validation, and reliability, tailored to the mechanical and electrochemical behavior of the CPEs. Properties of most inorganic solid electrolytes depend on the temperature and moisture; therefore, the tests are to be conducted at a controlled temperature and humidity in an argon-filled glove box or a dry room.

Cell testing and reporting require stringent regulations: Many laboratory experiments still operate at ultralow current densities, i.e., between 0.05 mA cm^{-2} and 0.2 mA cm^{-2} (equivalent to C/20 to C/10), which do not reflect realistic device usage. Zhang et al.^[28] recently showed that slow charging (0.2 C) and fast discharging (3 C) impressively improved the cycling stability of the Li//NCM cells filled with a highly concentrated liquid electrolyte compared to various other test conditions. A low rate charging during the formation cycle is also important for the stability of operation of the pouch cells using CPEs.^[29] However, similar studies for the solid-state cells are lacking;

Table 1. Currently adopted tests and recommended procedures for evaluation of ASSBs with CPEs.

Parameter	Current practice	Recommended standard
Temperature	Uncontrolled/ambience	$25\text{--}60 \pm 2$ [°C] with the measurement temperature specified
Humidity	Ambient lab air	RH $< 10\%$ (dry room or glove box)
Stack pressure	Mostly arbitrary	100 [kPa]–5 [MPa]
Current density	0.05–0.2 [mA·cm ⁻²] (0.1–0.05 [C])	Slow charging (0.2–1 [C]) Fast discharging (3–10 [C])
Cycle life testing	50–200 cycles at low C-rates	≥ 500 cycles at variable C-rates
Areal capacity	0.1–0.5 [mAh·cm ⁻²]	2–3 [mAh·cm ⁻²]
Charge/discharge cycling	Voltage controlled	Constant current + constant voltage during initial cycles, and constant current control subsequently
Abuse/safety testing	Cycling stability of the electrolyte using Li//Li symmetric cells	<ul style="list-style-type: none">• Thermal stability tests up to 150 [°C]• Mechanical deformation test: compression or puncture• Overcharge/overdischarge: to examine failure behavior• Short-circuit propagation: test for dendrite-induced failure under elevated current loads• Effect of humidity
Cell format	Coin cells	Full-sized pouch with tabs (100–200 [mAh])

therefore, following the above results, we assume a similar strategy could also work well for ASSBs. In short, for a real practical scenario, the charging should be at a current density in the $\approx 0.2\text{--}1 \text{ mA cm}^{-2}$ range and discharging at $\approx 3\text{--}10 \text{ mA cm}^{-2}$.

Charge polarization during charging and discharging events is an ongoing challenge in lithium-ion batteries; this issue is severe in CPEs due to orders of magnitude lower ionic conductivity in solid electrolytes than their liquid analogs. This causes large voltage drops and scattering across the electrolyte and interfaces, especially at higher current densities; therefore, the measured cell voltage does not always accurately reflect the true state of charge (SOC), and the familiar voltage profiles (like flat plateaus in NMC or graphite electrodes) become sloped or smeared, i.e., the cell may hit the cutoff voltage prematurely, even though capacity is not fully activated and utilized. This issue could be solved by a capacity-limited charge/discharge cycle so that the same amount of lithium is cycled each time, regardless of voltage noise from polarization. However, in early cycles, one may choose the voltage cutoffs to observe polarization behavior and get an estimate for the real limits; subsequently, as the interface is stabilized and the stack pressure is optimized, switch to capacity-based control for cycling consistency.

Analysis of cell failure conditions is among the stringent requirements for practical devices, and safety tests such as thermal abuse, short-circuit, or overcharge are rarely done in early research. While the Li//Li symmetric cells are routinely used for evaluating the stability of operation via determining the short circuits as well as the side reactions, operation under extreme conditions (failure analysis) such as thermal stability, effect of humidity, charge/discharge under extreme load, etc. are to be undertaken for leveraging the typical laboratory research leading to the technology readiness levels #3#4 into higher levels of scaling-up and testing under working conditions. Therefore, as proposed in the Table 1, the cells to be tested up to a temperature of $\approx 150^\circ\text{C}$, compression or puncture to test the mechanical stability of the devices, short-circuit propagation to test for dendrite-induced failure under elevated current loads, and overcharging and overdischarging to examine the cell failure

are among the recommended failure studies for solid state lithium-ion pouch cells.

3. Revision of Ionic Conductivity and Lithium Transference Numbers

The CPEs could be divided into two major categories, viz. solid (filler)-in-polymer and polymer-in-solid (filler), depending on the major phase. Polymer makes the major phase in the first category, and vice versa in the second category. The majority of the research volume on CPEs is on the solid-in-polymer category due to their superior mechanical properties and desirable ionic conductivity than the other. In experiments reported on the development of CPEs, weight fractions of the various components (polymer, filler, and lithium salt) are considered, but ignoring the fact that the volume fraction of the components and their distribution within the matrix for a percolative network is important for obtaining the composite properties. Considering the large difference in densities of polymers (typically ≈ 0.8 to 2.0 g cm^{-3}) and inorganic solids (typically ≈ 2 to 5 g cm^{-3}), their weight fraction mixture leads to a film with an island-like distribution of inorganic particles (fillers) in the sea of amorphized polymer network in the case of solid-in-polymer case (**Figure 2a**). This sporadic distribution of inorganic fillers within the polymer film has two consequences when the ion conduction through it is considered: i) the lithium cross-over cross-section (Pauling ionic radius of lithium is $\approx 60 \text{ pm}$) throughout the membrane is orders of magnitude lower than size of the inorganic nanosized particles (typically tens to hundreds of nanometers) and ii) the preference of the conducting ions to choose the path of lower resistance (following the Kirchhoff law). Consequently, in CPEs, lithium transport is significantly hindered due to i) limited percolation pathways in polymer-rich regions (**Figure 2a**),^[30–32] ii) strong ion-polymer interactions reduces the ion mobility,^[33,34] and iii) high resistance at polymer-inorganic interfaces.^[35–37] These observations are supported by the recent studies: i) spatially resolved conductivity measurements indicate highly non-uniform

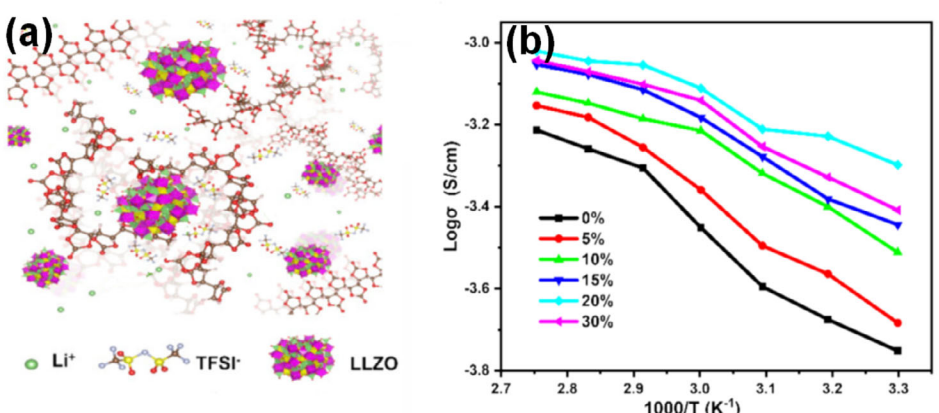


Figure 2. a) Cartoon depicting a typical CPE and b) electrical conductivity characteristic (Arrhenius curve) of a typical CPE containing polyvinylchloride (PVC) and LLZO with different LLZO contents. The lithium transport occurs through the interface region, polymer backbone, and inorganic solid. The data has been adopted from the ref. [49] with permission. Copyright (2025) Elsevier.

lithium transport pathways through CPEs;^[30,38] ii) *in situ* electron microscopy reveals localized lithium-ion depletion zones, contributing to performance degradation;^[39–42] and iii) simulated conductivity measurements based on realistic microstructures differ significantly from bulk measurements.^[43–45] These findings confirm that conventional measurement techniques provide an overly optimistic assessment of ionic transport in CPEs. Besides, the measured averaged conductivity through the entire volume of the CPE membrane did not account for the actual lithium diffusion path within it. Since conventional measurement methods assume a uniform transport environment, the measured ionic conductivity and transference number do not accurately reflect the true lithium-ion transport efficiency within the composite.

As stated, the ion conduction in CPEs could be deconvoluted into three processes, viz., i) ion hopping between the polar groups of the polymer (e.g., ether oxygens), ii) ion movement through the lattice vacancies in the inorganic phase, and iii) ion transport through the interface regions (Figure 2a). The ion movement in polymers is closely tied to local polymer chain mobility; therefore, the segmental motion of the polymer chains through the amorphous regions is the principal contributor to their ionic conductivity.^[46–48] Several vacancy-assisted transports through the inorganic electrolyte are evident such as ion-hopping through adjacent vacant sites and interstitials, interstitialcy (knock-on) mechanism (i.e., a migrating ion pushes a lattice ion from its site into a neighboring interstitial site, the host atom then pushes another atom, and so on), and ion conduction through the disordered grain boundaries. The space charge layers and Lewis acid-base interactions between the filler surface and polymer chains primarily contribute to the conductivity of the interface regions.^[46–48]

The lithium transference number (t_{Li^+}), i.e., the fraction of lithium ions transported through the membrane per ions that are generated, is an important quantity in CPEs, determining the storability and cyclability of the device. A high t_{Li^+} (ideally close to 1) is desirable because it signifies the absence of side reactions and can lead to superior battery performance by reducing the concentration polarization and improving the power density. In a solid electrolyte, anions (like $TFSI^-$ or PF_6^- in liquid electrolytes or lithium source additives) do not typically contribute to charge transport in the same way as lithium ions. Unlike liquid electrolytes, where both cations and anions migrate under an electric field, in solid polymer electrolytes and composite electrolytes, anions are often immobilized within the polymer matrix. This means that only lithium ions (Li^+) contribute to ionic conductivity, while charge neutrality is maintained by electrode reactions at the interfaces.

In routine laboratory experiments, the t_{Li^+} is determined using a combination of potentiostatic DC polarization and electrochemical impedance spectroscopy (EIS). These measurements are conducted using a symmetric Li/CPE/Li cell, where a small DC potential (10–50 mV) is applied, and the current response is monitored over time. The initial current (I_o) and steady-state current (I_{ss}) are recorded. EIS measurements are performed before and after polarization to determine the resistances (R_o and R_{ss}). Over time, the current decreases due to the polarization of mobile

species and eventually stabilizes. The t_{Li^+} is calculated using the following equation

$$t_{Li^+} = \frac{I_{ss}(\Delta V - I_o R_o)}{I_o(\Delta V - I_{ss} R_{ss})} \quad (1)$$

While this equation holds good for chemically homogeneous electrolytes (e.g., solid polymer electrolytes or pure inorganic electrolytes), to account for the difference in ionic conductivities between the solid electrolyte (σ_{SE}) and polymer electrolyte (σ_p) in CPEs, we need to modify the equation by incorporating the effective transport properties of each phase.

A model to evaluate t_{Li^+} considering the above limitations is presented herewith, taking the difference in conductivities into account (Figure 2), the electrical percolation between the components forming the electrolyte, and the Nernst-Einstein equation.

The total effective ionic conductivity (σ_{eff}) of a CPE, considering the above detailed transport mechanisms, can be written as

$$\sigma_{eff} = \sigma_p \phi_p + \sigma_{SE} \phi_{SE} + \sigma_{int} \phi_{int} \quad (2)$$

where, σ_p , σ_{SE} , and σ_{int} are the conductivities of the polymer, solid (inorganic, filler) electrolyte, and interfacial regions, respectively, and ϕ_p , ϕ_{SE} , and ϕ_{int} are their corresponding volume fractions. This equation assumes a homogeneous distribution of conductive pathways through respective phases. However, in practical CPEs, microstructural variations can lead to material-dependent ion transport. To account for this, percolation theory could be applied,^[49–51] which can be expressed as

$$\sigma_{eff} = \sigma_{SE} \left(\frac{\phi_{SE} - \phi_c}{1 - \phi_c} \right)^n \quad (3)$$

where ϕ_c is the critical percolation threshold, i.e., the minimum volume fraction of the solid electrolyte needed to form a continuous conductive network, and n is an empirical exponent that depends on the dimensionality and connectivity of the composite and can be obtained from conductivity versus volume fraction measurements. This model indicates that effective ionic conductivity significantly increases when the solid electrolyte content surpasses the percolation threshold, forming continuous ion-conducting pathways. However, solid particles content in a polymeric network above a certain threshold compromises the mechanical flexibility of the electrolyte membrane.

The ionic conductivity (σ) to the diffusion coefficient (D), charge (z), and concentration (c) of mobile ions are related through the Nernst-Einstein equation as

$$\sigma = \frac{z^2 F^2}{RT} D c \quad (4)$$

Substituting and simplifying

$$t_{Li^+} = \frac{I_{ss}}{I_{total}} = \frac{D_{Li^+} c_{Li^+}}{D_{Li^+} c_{Li^+} + D_{anion} c_{anion}} \quad (5)$$

In composite electrolytes, lithium-ion conduction occurs through both polymer (p) and solid electrolyte (SE) phases and

their interfaces. Applying the Nernst–Einstein equation to the lithium-ion conduction

$$t_{\text{Li}^+}^{\text{eff}} = \frac{D_{\text{Li}^+}^{\text{P}} \phi_{\text{p}} + D_{\text{Li}^+}^{\text{SE}} \phi_{\text{SE}}}{D_{\text{Li}^+}^{\text{P}} \phi_{\text{p}} + D_{\text{Li}^+}^{\text{SE}} \phi_{\text{SE}} + D_{\text{trap}} \phi_{\text{trap}}} \quad (6)$$

where $D_{\text{Li}^+}^{\text{P}}$ and $D_{\text{Li}^+}^{\text{SE}}$ are the lithium-ion diffusion coefficients in the polymer and solid electrolyte phases, respectively, with their respective phase volume fractions ϕ_{p} and ϕ_{SE} . D_{trap} and ϕ_{trap} account for lithium ions immobilized due to interactions with the polymer matrix or interfacial trapping and its phase volume fraction, respectively. Considering the major conducting phases in the CPE, the effective conductivity can be written as

$$\sigma_{\text{eff}} = \sigma_{\text{p}} \phi_{\text{p}} + \sigma_{\text{SE}} \phi_{\text{SE}} \quad (7)$$

To modify the transference number equation, we assume that the initial and steady-state currents are affected by the relative conductivities of each phase ($\sigma_r \phi_r$, where r is any phase). Considering the two types of CPEs, i.e., solid-in-polymer and polymer-in-solid, the correction term to the lithium transference number can be applied separately. For the first case (solid-in-polymer), polymer forms the major phase (i.e., $\phi_{\text{p}} \gg \phi_{\text{SE}}$) and the reverse holds for the polymer-in-solid case. The modified lithium transference number can be expressed as, respectively, for the solid-in-polymer (Equation (8)) and the polymer-in-solid (Equation (9)) as

$$t_{\text{Li}^+} = \frac{I_{\text{ss}}(\Delta V - I_o R_o)}{I_o(\Delta V - I_{\text{ss}} R_{\text{oss}})} \times \frac{\sigma_{\text{p}} \phi_{\text{p}} + \sigma_{\text{SE}} \phi_{\text{SE}}}{\sigma_{\text{SE}} \phi_{\text{SE}}} \quad (8)$$

$$t_{\text{Li}^+} = \frac{I_{\text{ss}}(\Delta V - I_o R_o)}{I_o(\Delta V - I_{\text{ss}} R_{\text{oss}})} \times \frac{\sigma_{\text{p}} \phi_{\text{p}} + \sigma_{\text{SE}} \phi_{\text{SE}}}{\sigma_{\text{p}} \phi_{\text{p}}} \quad (9)$$

The term $\frac{\sigma_{\text{p}} \phi_{\text{p}} + \sigma_{\text{SE}} \phi_{\text{SE}}}{\sigma_{\text{X}} \phi_{\text{X}}}$ accounts for the contribution of both the polymer and solid electrolyte to the total ionic conductivity. Since solid electrolytes generally have higher conductivity than polymers, this correction adjusts the lithium transference number to reflect the real contribution of lithium-ion transport in a heterogeneous medium.

Equation (8) and (9) imply that i) if ϕ_{SE} is high and a percolating network forms, lithium transport is dominated by the solid inorganic electrolyte and $t_{\text{Li}^+} \approx 1$; ii) if ϕ_{p} is high and lithium moves through the polymer, σ_{p} dominates and t_{Li^+} decreases; and iii) if the composite electrolyte has poorly connected phases, interfacial resistance further reduces effective t_{Li^+} . When the solid electrolyte dominates ($\phi_{\text{SE}} \rightarrow 1, \sigma_{\text{SE}} \gg \sigma_{\text{p}}$), the correction factor approaches unity, and the equation reduces to the original form. When the polymer-rich phase dominates ($\phi_{\text{p}} \rightarrow 1, \sigma_{\text{p}}$ is small), lithium-ion transport is more hindered and t_{Li^+} decreases. The equation provides a more realistic estimation of t_{Li^+} by incorporating heterogeneous ion conduction pathways.

Nevertheless, Equation (8) and (9) are valid only within the percolation limits. A survey of literature shows that systematic quantifications are not followed in the CPE research including i) electrical percolation and transport are not addressed, ii) mostly the weight fractions are considered without providing the actual

quantities of polymers and fillers considered during the work, and iii) a standard protocol for testing and reporting are not followed. Lack of such systematicity leads to unverifiable results; for example, Shi et al.^[52] prepared a CPE using gallium doped LLZO (LGLZO) in different weight percentages (0–30 wt%) in poly(vinylene carbonate) (PVC, $\sigma \approx 3.16 \times 10^{-6} \text{ S cm}^{-1}$) and found that the ionic conductivity enhancements were only up to 20 wt% of the inorganic filler (LGLZO) ($\sigma \approx 5 \times 10^{-4} \text{ S cm}^{-1}$) (Figure 2b). Beyond this threshold, the LGLZO agglomerated and reduced the conductivity. The t_{Li^+} value calculated using Equation (1) for the PVC-20wt.%LGLZO was ≈ 0.616 , which was significantly higher than common liquid electrolyte (LiPF_6 in EC/EMC/DMC; $t_{\text{Li}^+} \approx 0.38$). While the symmetrical lithium cell constituting the PVC-20wt.%LGLZO CPE could be cycled (lithium plating/stripping) over 500 h, the electrolyte membrane without LGLZO failed at ≈ 350 h. A full cell using LiFePO_4 has also been shown to be stable over 100 cycles at 0.2 C. As the quantity of materials in the CPE has not been reported, Equation (8) and (9) could not be verified. Further, how a device using the liquid electrolyte performs under similar fabrication and testing conditions also has not been undertaken.

Potential materials remedies to address the ionic conductivity and lithium transference number of CPEs with the help of the corrected equations are (i) optimizing microstructure by introducing nanoscale solid electrolytes to enhance percolation or engineering polymer-ceramic interfaces to reduce resistance or developing hierarchical architectures (such as nanowires or nanosheets) for more uniform ion transport by reducing the percolation threshold; (ii) advanced characterization techniques by using spatially resolved impedance spectroscopy or conducting operando neutron scattering and NMR to track lithium diffusion; and (iii) improved electrolyte design to incorporate highly conductive polymer electrolytes or utilizing functional additives to modulate lithium solvation environments. Nevertheless, this study identifies the need for standard testing and reporting conditions for meaningful comparison and further growth of the research area for realizing all solid-state secondary batteries.

4. Conclusions

In conclusion, this article addresses two important issues in all-solid-state lithium-ion batteries employing a composite polymer electrolyte, viz., i) a standard protocol for fabrication, testing, and reporting testing and ii) corrected model for evaluation of lithium transference number considering the percolation theory and difference in ionic conductivity between the inorganic and polymeric ionic conductors. Considering the advantages of pouch cells toward efficiencies, packing efficiency, and thermal management, they should be the standard cells for reporting. The thickness of the electrolyte and lithium electrode are recommended to be < 100 and $20 \mu\text{m}$, respectively, based on our literature review. Besides, a stack pressure of $\approx 100 \text{ kPa}–5 \text{ MPa}$, depending on the relative fractions of polymer and filler (inorganic electrolyte), is an important fabrication parameter to minimize the risk of lithium dendrites, control swelling, and ensure cell integrity. Measurement of cell properties also requires

strict regulations considering the humidity and temperature dependence of the composite polymer electrolyte film. Slow charging ($0.2\text{--}1\text{ mA cm}^{-2}$) and fast discharging ($3\text{--}10\text{ mA cm}^{-2}$) are shown to be ideal for cell longevity.

Further, we present a corrected equation to calculate the lithium transference number of composite polymer electrolytes, considering the relative fractions of the polymer and solid electrolyte as an effort to address the failure of ASSBs employing composite polymer electrolytes. Conventionally, the average ionic conductivity and the lithium transference number is overestimated as i) the model so far did not account the smaller lithium cross-over cross section as size of Li^+ is much smaller than the size of the inorganic solid electrolytes, ii) the transporting ions choose the path of highly conducting domains, and iii) the percolation behavior of the inorganic–polymer composite is rarely addressed. More accurate transport models, advanced characterization methods, and rational electrolyte design are crucial to overcoming these challenges. By addressing these limitations, long-term cycling stability and practical implementation of CPE-based ASSBs can be significantly improved.

Acknowledgements

This work is supported by the National Science and Technology Council, Taiwan, through the grant NSTC 114 2222 E 131 001 MY3. Authors are thankful to the solid-electrolyte group of the Battery Research Center of Clean Energy, Ming Chi University of Technology.

Conflict of Interest

The authors declare no conflict of interest.

Keywords: fabrication standards • ion transport • lithium metal batteries • pouch cells • solid state devices

- [1] B. Zhang, Z. Lin, H. Dong, L.-W. Wang, F. Pan, *J. Mater. Chem. A* **2020**, *8*, 342.
- [2] X. Tao, L. Yang, J. Liu, Z. Zang, P. Zeng, C. Zou, L. Yi, X. Chen, X. Liu, X. Wang, *J. Alloys Compd.* **2023**, *937*, 168380.
- [3] J. Sastre, A. Priebe, M. Döbeli, J. Michler, A. N. Tiwari, Y. E. Romanyuk, *Adv. Mater. Interfaces* **2020**, *7*, 2000425.
- [4] R. Gu, J. Kang, X. Guo, J. Li, K. Yu, R. Ma, Z. Xu, L. Jin, X. Wei, *J. Alloys Compd.* **2022**, *896*, 163084.
- [5] Q. Y. Wu, D. Y. Zheng, R. Y. Mao, C. Liu, X. Wang, W. B. Han, *AlP Adv.* **2023**, *13*.
- [6] D. Liu, W. Zhu, Z. Feng, A. Guerfi, A. Vijh, K. Zaghib, *Mater. Sci. Eng. B* **2016**, *213*, 169.
- [7] L. Schweiher, K. Hogrefe, B. Gadermaier, J. L. M. Rupp, H. M. R. Wilkening, *J. Am. Chem. Soc.* **2022**, *144*, 9597.
- [8] Z. Wu, H. Tian, D. Ji, X. Zhang, L. Li, Z. Lou, W. Sun, M. Gao, Y. Liu, H. Pan, *J. Energy Chem.* **2025**, *105*, 713.
- [9] X. Zhang, S. Cheng, C. Fu, G. Yin, L. Wang, Y. Wu, H. Huo, *Nano-Micro Lett.* **2025**, *17*.
- [10] Y.-L. Liao, X.-L. Wang, H. Yuan, Y.-J. Li, C.-M. Xu, S. Li, J.-K. Hu, S.-J. Yang, F. Deng, J. Liu, J.-Q. Huang, *Adv. Mater.* **2025**, *37*, 2419782.
- [11] L. Wang, L. Xie, Y. Song, X. Liu, H. Zhang, X. He, *Energy* **2023**, *2*, 20220025.
- [12] E. Fedeli, O. Garcia-Calvo, A. Gutiérrez-Pardo, T. Thieu, I. Combarro, R. Paris, J. Nicolas, H.-J. Grande, I. Urdampilleta, A. Kvasha, *Solid State Ion.* **2023**, *392*, 116148.
- [13] W. Lee, J. Lee, T. Yu, H.-J. Kim, M. K. Kim, S. Jang, J. Kim, Y.-J. Han, S. Choi, S. Choi, T.-H. Kim, S.-H. Park, W. Jin, G. Song, D.-H. Seo, S.-K. Jung, J. Kim, *Nat. Commun.* **2024**, *15*, 5860.
- [14] J. You, Q. Wang, R. Wei, L. Deng, Y. Hu, L. Niu, J. Wang, X. Zheng, J. Li, Y. Zhou, J.-T. Li, *Nano-Micro Lett.* **2024**, *16*, 257.
- [15] F.-f. Bai, M.-b. Chen, W.-j. Song, Y. Li, Z.-p. Feng, Y. Li, *Energy Proc.* **2019**, *158*, 3682.
- [16] Kaushubharam, P. K. Koorata, S. Panchal, R. Fraser, M. Fowler, *J. Energy Storage* **2024**, *84*, 110928.
- [17] H. Chang, X. Zhang, W. Li, H. Liu, H. Hu, Z. Liu, W. Liu, Y. Jin, *Materials* **2025**, *6*, 100307.
- [18] Y.-J. Lee, S.-B. Hong, H.-J. Lee, H.-T. Sim, Y. Kim, S. Kim, D.-W. Kim, *Chem. Eng. J.* **2023**, *477*, 146983.
- [19] A. Kubanska, L. Castro, L. Tortet, M. Dollé, R. Bouchet, *J. Electroceram.* **2017**, *38*, 189.
- [20] J. Lee, S. H. Jeong, J. S. Nam, M. Sagong, J. Ahn, H. Lim, I.-D. Kim, *EcoMat*, **2023**, *5*, e12416.
- [21] X. Zhang, C. Luo, N. Menga, H. Zhang, Y. Li, S.-P. Zhu, *Science* **2023**, *4*, 101328.
- [22] Y. Ren, W. Shin, A. Manthiram, *Adv. Energy Mater.* **2022**, *12*, 2200190.
- [23] J. Lee, H. R. Shin, M. Han, M. Ryu, B. Kim, H. Jung, J.-H. Choi, K.-N. Jung, J.-W. Lee, J. Lee, *J. Energy Storage* **2025**, *118*, 116307.
- [24] C. Lee, J. Y. Kim, K. Y. Bae, T. Kim, S.-J. Jung, S. Son, H.-W. Lee, *Energy Storage Mater.* **2024**, *66*, 103196.
- [25] A. Schommer, M. O. Corzo, P. Henshall, D. Morrey, G. Collier, *J. Power Sources* **2025**, *629*, 236019.
- [26] P. Roering, G. M. Overhoff, K. L. Liu, M. Winter, G. Brunklaus, *ACS Appl. Mater. Interfaces* **2024**, *16*, 21932.
- [27] J. Min, Z. Liang, N. F. Pietra, C. Connor, L. A. Madsen, F. Lin, *ACS Appl. Mater. Interfaces* **2025**, *17*, 36639-36649.
- [28] Y. Zhang, W. Bao, E. Jeffs, B. Liu, B. Han, W. Mai, X. Li, W. Li, Y. Xu, B. Bhamwala, A. Liu, L. Ah, K. Ryu, Y. S. Meng, H. Gan, *ACS Energy Lett.* **2025**, *10*, 872.
- [29] S. Kim, P. N. Didwal, J. Fiates, J. A. Dawson, R. S. Weatherup, M. De Volder, *ACS Energy Lett.* **2024**, *9*, 4753.
- [30] A. Mascaro, Z. Wang, P. Hovington, Y. Miyahara, A. Paoletta, V. Gariepy, Z. Feng, T. Enright, C. Aiken, K. Zaghib, K. H. Bevan, P. Grutter, *Nano Lett.* **2017**, *17*, 4489.
- [31] Y. Zeng, D. Chalise, Y. Fu, J. Schaadt, S. Kaur, V. Battaglia, S. D. Lubner, R. S. Prasher, *Joule* **2021**, *5*, 2195.
- [32] C. Huang, M. D. Wilson, B. Cline, A. Sivarajah, W. Stolp, M. N. Boone, T. Connolley, C. L. A. Leung, *Cell Rep. Phys. Sci.* **2024**, *5*, 101995.
- [33] Y. Luo, L. Gao, W. Kang, *J. Energy Chem.* **2024**, *89*, 543.
- [34] N. S. Schausier, R. Seshadri, R. A. Segelman, *Mol. Syst. Des. Eng.* **2019**, *4*, 263.
- [35] J. Pan, P. Zhao, N. Wang, F. Huang, S. Dou, *Energy Environ. Sci.* **2022**, *15*, 2753.
- [36] E. Kuhnert, L. Ladenstein, A. Jodlbauer, C. Slugovc, G. Trimmel, H. M. R. Wilkening, D. Rettenwander, *Cell Rep. Phys. Sci.* **2020**, *1*, 100214.
- [37] M. J. Counihan, J. Lee, P. Mirmira, P. Barai, M. E. Burns, C. V. Amankukwu, V. Srinivasan, Y. Zhang, S. Tepavcevic, *Energy Mater.* **2025**, *5*, 500032.
- [38] J. H. Thienenkamp, P. Lennartz, M. Winter, G. Brunklaus, *Cell Rep. Phys. Sci.* **2024**, *5*, 102340.
- [39] D. Chen, S. Idris, M. Schulz, B. Gamer, R. Möning, *J. Power Sources* **2011**, *196*, 6382.
- [40] J. Woods, N. Bhattacharai, P. Chapagain, Y. Yang, S. Neupane, *Nano Energy* **2019**, *56*, 619.
- [41] Y. Cheng, L. Zhang, Q. Zhang, J. Li, Y. Tang, C. Delmas, T. Zhu, M. Winter, M.-S. Wang, J. Huang, *Mater. Today* **2021**, *42*, 137.
- [42] X. H. Liu, J. Y. Huang, *Energy Environ. Sci.* **2011**, *4*, 3844.
- [43] M. A. S. Matos, V. L. Tagarielli, S. T. Pinho, *Compos. Sci. Technol.* **2020**, *188*, 108003.
- [44] M. Neumann, O. Stenzel, F. Willot, L. Holzer, V. Schmidt, *Int. J. Sol. Struct.* **2020**, *184*, 211.
- [45] O. Stenzel, O. Pecho, L. Holzer, M. Neumann, V. Schmidt, *AIChE J.* **2017**, *63*, 4224.
- [46] Z. Li, J. Fu, X. Zhou, S. Gui, L. Wei, H. Yang, H. Li, X. Guo, *Adv. Sci.* **2023**, *10*, 2201718.

- [47] J. Fu, Z. Li, X. Zhou, X. Guo, *Mater. Adv.* **2022**, *3*, 3809.
- [48] H. Gudla, A. Hockmann, D. Brandell, J. Mindemark, *Materials* **2025**, *7*, 4716.
- [49] S. Jiang, J. B. Wagner, *J. Phys. Chem. Solids* **1995**, *56*, 1113.
- [50] H. Yuan, H. Chen, M. Li, L. Liu, Z. Liu, *Soft Matter* **2023**, *19*, 7149.
- [51] M. Mazaheri, J. Payandehpeyman, S. Jamasb, *Appl. Compos. Mater.* **2022**, *29*, 695.
- [52] W. Shi, S. Cao, G. Zhang, C. Mao, X. Dai, G. Yin, F. Chen, *Solid State Ion.* **2025**, *420*, 116771.

Manuscript received: April 19, 2025
Revised manuscript received: July 3, 2025
Version of record online:
